Multi-User Position Estimation and Performance Trade-offs in IEEE 802.11az WLANs

Varun Amar Reddy and Gordon L. Stüber, *Fellow, IEEE*

***Abstract*—Location-Based Services (LBSs) using wireless communication systems have witnessed a dramatic increase in both demand and applicability. In particular, there is a need for high-accuracy position estimation in dense indoor environments, while sustaining data communication services. In this paper, analytical expressions are formulated to characterize the trade-off between the position estimation accuracy and the latency/throughput performance in a multi-user IEEE 802.11az scenario. Furthermore, optimization frameworks are developed using which the proposed enhancements can tune the degree of trade-off, in terms of the number of preamble symbol repetitions. The impact of the desired position accuracy, Signal-to-Noise Ratio (SNR), bandwidth, and user-grouping strategies are evaluated as well.**

***Index Terms*—preamble design, wireless LAN, IEEE 802.11az, position estimation, latency, throughput, multi-user MIMO, OFDMA, optimization.**

I. Introduction

Over the past few years, the prevalence of wireless-enabled Location-Based Services (LBSs) has increased with the rise of Internet-of-Things (IoT) and a surge in the number of end-user devices such as smartphones. Such LBSs have been applied to a variety of sectors, ranging from inventory and warehouse management to assistive healthcare [1]. While several positioning solutions, such as GPS and wide-area LTE, have been in use, their efficacy is lowered in indoor and dense urban environments. Moreover, the current trend has been to incorporate positioning capability into indoor technologies, such as IEEE 802.11 for Wireless Local Area Networks (WLANs). The IEEE 802.11az standard [2] is one such significant effort towards enhancing position estimation performance using WiFi infrastructure that is prevalent in indoor environments.

Various works have laid the foundation for position estimation and establishing performance limits [1], [3]. However, relatively fewer works have analyzed the performance of the upcoming positioning enhancements to IEEE 802.11. A passive positioning method was proposed in [4] on the basis of the Fine Timing Measurement (FTM) scheme employed in IEEE 802.11. The use of IEEE 802.11az in an IoT scenario was evaluated in [5]. Computation of the anchor positions and other security aspects were studied in [6].

While the above works have considered the problem of position estimation alone, the crucial motivation for this work arises from the fact that the introduction of positioning services would restrain the resources allocated to data communication services. To the best of the authors' knowledge, this is the first work that analyzes the trade-off between latency/throughput performance and multi-user position estimation accuracy in IEEE 802.11az WLANs. Analytical expressions are derived for the position error bounds, latency, and throughput. Furthermore, optimization problems are formulated and solved for the optimal number of preamble symbol repetitions that minimizes the latency (or maximizes the throughput) under position accuracy constraints.

This work was performed by the authors at the Georgia Institute of Technology, Atlanta, GA 30332, USA.

V. A. Reddy is a senior systems engineer with the Qualcomm Wireless Research group in San Diego, CA 92121, USA (e-mail: varunama@qti.qualcomm.com).

G. L. Stüber is with the School of Electrical and Computer Engineering, Georgia Institute of Technology, Atlanta, GA 30332, USA (e-mail: stuber@ece.gatech.edu).

II. Overview of range estimation in IEEE 802.11

The Fine Timing Measurement (FTM) protocol was developed by the IEEE 802.11mc working group [4]. The overall idea is to obtain timestamps of packets that are exchanged between an Initiating Station (ISTA) and a Responding Station (RSTA). Typically, in a given Basic Service Set (BSS), the Access Points (APs) serve as RSTAs whose positions are known. An FTM session is triggered by the transmission of an FTM request, which is used to negotiate the Physical (PHY) and Medium Access Control (MAC) layer parameters that will be employed during the FTM session. As shown in Fig. 1, ranging frames are exchanged between the ISTA and RSTA, which enable the estimation of the Round-Trip Time (RTT) and consequently, the distance between the nodes (R).

$$\text{RTT} = (t_4 - t_1) - (t_3 - t_2) \tag{1}$$

$$R = \left(\frac{\text{RTT}}{2}\right) \cdot c \tag{2}$$

where c denotes the speed of light. When at least three unique measurements are made between the ISTA and RSTAs, the ISTA can estimate its position.

A. IEEE 802.11az

The upcoming IEEE 802.11az standard introduces various enhancements to the FTM protocol [2]. A significant enhancement is the introduction of a Trigger-based (TB) ranging scheme that enables multi-user positioning via Orthogonal

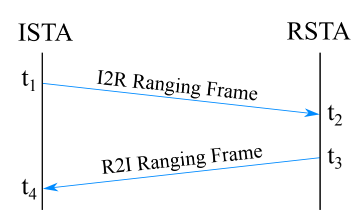

Fig. 1: Two-way ranging between an ISTA and RSTA.

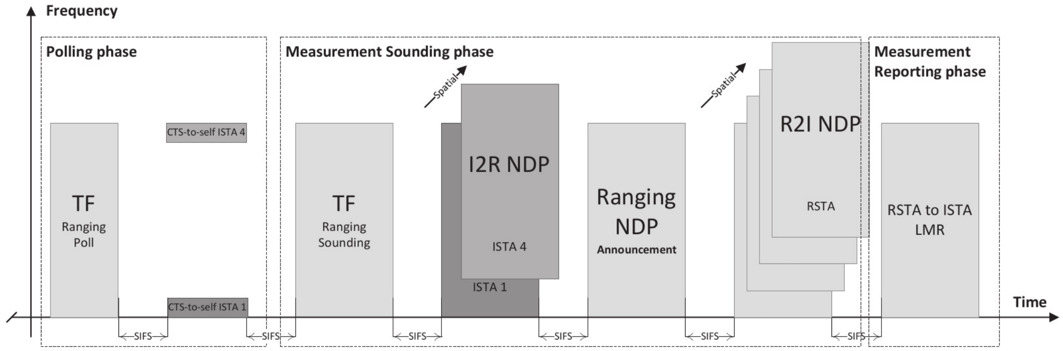

Fig. 2: Operation of TB ranging in the case of four ISTAs [2].

Frequency Division Multiple Access (OFDMA) and Multi-User Multiple-Input Multiple-Output (MU-MIMO). A detailed working of the TB ranging protocol is illustrated in Fig. 2.

1) During the polling phase, the RSTA broadcasts a Trigger Frame (TF) Ranging Poll to confirm which of the ISTAs will be participating in the positioning session. Note that the STAs acknowledge and respond using OFDMA.
2) During the sounding phase, a TF Ranging Sounding frame is transmitted by the RSTA to trigger the transmission of sounding frames from the ISTAs, using multi-user MIMO. With reference to Fig. 2, the I2R frames help determine t_1 and t_2 for each of the ISTAs.
3) This is acknowledged by the RSTA, following which an R2I frame is transmitted on the downlink to help determine t_3 and t_4 for each of the ISTAs.
4) During the final reporting phase, the RSTA provides its measurements to the ISTAs in a Location Measurement Report (LMR) frame, so that they may estimate the RTT.

III. Trade-off Analysis and Proposed Enhancements

The above TB ranging scheme is employed in conjunction with the exchange of regular frames pertaining to data communication services. Hence, providing positioning services implies a reduction of the overall throughput or an increase in the latency. The IEEE 802.11az standard allows an ISTA-RSTA pair to negotiate on the number of preamble symbol repetitions (N), which provides a way to tweak the level of trade-off between attaining better SNR and position estimation accuracy and requiring a larger allocation of time resources.

A. Proposed enhancements

Consider an infrastructure of RSTAs that provide both data and ranging services. A group of ISTAs that are associated with one of the RSTAs (say 'A'), is capable of exchanging data only with A, while it can perform ranging measurements with the entire infrastructure.

The following sequence of steps can enable an optimization of the trade-off between the latency, throughput and positioning accuracy performance.

- A maintains a list of requirements desired by the ISTAs, pertaining to parameters such as the ranging accuracy, latency, and throughput.
- In parallel, A also communicates with the backbone infrastructure and maintains a list of other RSTAs that can provide ranging services to the same ISTAs, along with the corresponding Signal-to-Noise Ratio (SNR) values perceived by the RSTAs.
- A optimizes the number of symbol repetitions (for each of the ISTA-RSTA pairs) so as to meet the desired requirements.
- The RSTAs trigger ranging sessions with the ISTAs as per the configuration parameters provided by A. Meanwhile, the ISTAs exchange data packets with A.

In the following subsections, an analytical model is developed for the position error bound under the TB ranging scheme, following which an optimization framework is formulated and solved, in line with the aforementioned enhancements/scheme.

B. Position Error Bounds

The Time-of-Arrival (ToA) estimation procedure for an OFDM-based IEEE 802.11 receiver is described in [2], [7]. A coarse estimate is obtained as the delay that yields a peak in the cross-correlation between the received signal and the known preamble sequence. Sub-sample corrections are made to the coarse estimate by analysing the mean phase shift between the subcarriers. Let $\mathbf{h} \in \mathbb{C}^{K\times 1} = [h_1 \; h_2 \; \cdots \; h_K]$ denote the channel estimate for a single spatial stream between an RSTA and an ISTA, where K is the total number of subcarriers. Given that Δf denotes the subcarrier spacing, the fine ToA adjustment τ is given by

$$\tau = \frac{1}{2\pi(K-1)\Delta f}\sum_{k=1}^{K-1} \angle h_k - \angle h_{k+1} \tag{3}$$

Through this approach, the Cramér-Rao Bound (CRB) on the range estimate is expressed as [7]

$$\mathrm{CRB}_r = \frac{c^2}{8N\pi^2 K\gamma\beta^2} \tag{4}$$

where γ denotes the mean SNR per subcarrier and β is the baseband effective bandwidth [3].

Consider the aforementioned RTT estimation procedure in Section II-A between the i^{th} ISTA and j^{th} RSTA. Let $N_{\mathrm{I},i,j}$ and $N_{\mathrm{R},i,j}$ denote the number of symbol repetitions in the I2R and R2I frames respectively. Following the analysis in [8] for a two-way ranging scheme, the variance of the range estimate using the described RTT-based method is derived as

$$\sigma^2_{(i,j)} = \left(\frac{1}{N_{\text{I},i,j}} + \frac{1}{N_{\text{R},i,j}}\right) \frac{c^2}{16\pi^2 K \gamma_{(i,j)} \beta^2} \tag{5}$$

Given three RSTAs, whose positions are known, the resultant CRB and Position Error Bound (PEB) for the i^{th} ISTA are given by

$$\text{CRB}_i = \text{tr}\left\{\left(\mathbf{J}_i \mathbf{F}_i \mathbf{J}_i^{\text{H}}\right)^{-1}\right\} \tag{6}$$

$$\text{PEB}_i = \sqrt{\text{CRB}_i} \tag{7}$$

$$\mathbf{F}_i = \begin{pmatrix} \sigma^{-2}_{(i,1)} & 0 & 0 \\ 0 & \sigma^{-2}_{(i,2)} & 0 \\ 0 & 0 & \sigma^{-2}_{(i,3)} \end{pmatrix} \tag{8}$$

$$\mathbf{J}_i = \begin{pmatrix} \frac{x_i - x'_1}{d_{i,1}} & \frac{x_i - x'_2}{d_{i,2}} & \frac{x_i - x'_3}{d_{i,3}} \\ \frac{y_i - y'_1}{d_{i,1}} & \frac{y_i - y'_2}{d_{i,2}} & \frac{y_i - y'_3}{d_{i,3}} \end{pmatrix} \tag{9}$$

where (x_i, y_i) and (x'_j, y'_j) are the true positions of the i^{th} ISTA and the j^{th} RSTA respectively, and $d_{i,j}$ is the distance between them.

C. Analytical expressions

In this section, formulations are derived for the latency and the throughput in a multi-user scenario. The total time required by the i^{th} ISTA to complete a ranging session with the j^{th} RSTA (as per Fig. 2) can be expressed as

$$t_{r,j} = t_{\text{TF}} + t_{\text{CTS}} + 2 \cdot \text{SIFS} + \max\{t_{\text{I2R},i,j}\} + t_{\text{R2I},j} + t_{\text{LMR}} \tag{10}$$

$$t_{\text{I2R},i,j} = t_{\text{TF}} + 2 \cdot \text{SIFS} + t_h + 8 \cdot S_{i,j} \cdot N_{\text{I},i,j} \tag{11}$$

$$t_{\text{R2I},j} = t_{\text{NDPA}} + 2 \cdot \text{SIFS} + t_h + \sum_{i=1}^{I} 8 \cdot S_{i,j} \cdot N_{\text{R},i,j} \tag{12}$$

where the various notations are specified in Table I, and the time durations are represented in microseconds. Note that there are multiple I2R packets being transmitted on the uplink by various ISTAs, while a single R2I packet is sent on the downlink by the RSTA.

Consider the following formulations for the overall latency ($\mathcal{L}$) and throughput ($\mathcal{T}$) in completing a positioning session with J RSTAs and data transmission on the downlink (using either OFDMA or MU-MIMO).

$$\mathcal{L} = \sum_{j=1}^{J} (t_{r,j}) + t_D \tag{13}$$

$$\mathcal{T} = \frac{\sum_{i=1}^{I} \sum_{s=1}^{S_i} D_{s,i}}{\sum_{j=1}^{J} (t_{r,j}) + t_D} \tag{14}$$

TABLE I: List of notations.

Notation	Description
I	Total number of ISTAs
S_i	Number of spatial streams allocated to the i^{th} ISTA
t_{TF}	Time duration of a trigger frame
t_{CTS}	Time duration of a Clear-To-Send frame
SIFS	Short Interframe Spacing
t_{LMR}	Time duration of a Location Measurement Report frame
t_{NDPA}	Time duration of a Null Data Packet Announcement frame
t_h	Time duration of the header portion of an I2R/R2I frame
t_D	Time duration of the downlink data packet
$D_{s,i}$	Amount of data corresponding to the s^{th} spatial stream of the i^{th} ISTA

D. An Optimization Framework

Optimization problems with the objective of minimizing the latency or maximizing the throughput, can be constructed by imposing a minimum user-specific ranging accuracy constraint. On the uplink, it can be observed that each ISTA sends its own frame, whose transmissions are coordinated using MU-MIMO. Overall, the effect is that the ISTA that imposes the longest frame duration becomes the duration of the overall I2R frame. Hence, the RSTA may simply apply a common value for the number of symbol repetitions across all the ISTAs. This implies that

$$\max\{t_{\text{I2R},i,j}\} = t_{\text{TF}} + 2 \cdot \text{SIFS} + t_h + 8 \cdot \max\{S_{i,j}\} \cdot N_{\text{I},j} \tag{15}$$

$$N_{\text{I},i,j} = N_{\text{I},j} \quad \forall i \tag{16}$$

Based on the foregoing analysis, consider the following latency minimization problem -

$$\underset{[N_{\text{I},j},\ N_{\text{R},1,j} \cdots N_{\text{R},I,j}]}{\text{minimize}} \quad \mathcal{L} \qquad \forall i, j \tag{17}$$

$$\sigma^2_{(i,j)} \geq \sigma_{i,0} \qquad \forall i, j \tag{18}$$

$$1 \leq N_{\text{I},j} \leq 8 \qquad \forall j \tag{19}$$

$$1 \leq N_{\text{R},i,j} \leq 8 \qquad \forall i, j \tag{20}$$

$$N_{\text{I},j},\ N_{\text{R},i,j} \in \mathbb{N} \qquad \forall i, j \tag{21}$$

where (18) imposes a minimum value on the ranging accuracy for a given ISTA-RSTA pair, and (19)-(21) impose an integer-interval constraint on the number of symbol repetitions [2]. The convexity of a relaxed version of the problem (without integer constraints) is straightforward to note. This is implied by the fact that the objective function in (17) is a linear combination of the variables, while the constraint in (18) is a linear combination of the inverse of two positive variables [9]. The above constraints and analysis apply to the throughput maximization problem as well.

There exist several techniques to rapidly solve such convex mixed-integer non-linear programs [10], particularly since the sample space is relatively small in size (inferred from (19)-(21)).

IV. Performance Evaluation

The performance of the proposed scheme is evaluated as a function of the position accuracy desired by the ISTAs. The

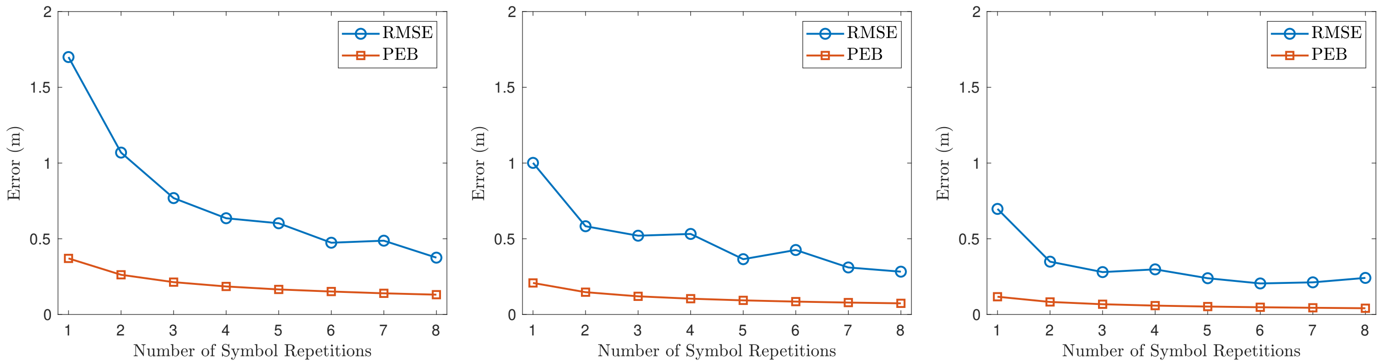

(a) SNR = 10 dB.

(b) SNR = 15 dB.

(c) SNR = 20 dB.

Fig. 3: A comparison between the RMSE error and the PEB as a function of the average SNR per symbol.

effect of the average SNR per symbol, the resultant Modulation and Coding Scheme (MCS), and the bandwidth allocated to each of the ISTAs is analyzed as well.

A. Simulation Setup

Consider a group of 4 ISTAs being serviced by 3 RSTAs, where each ISTA is associated with its own level of SNR and bandwidth allocation. The various simulation parameters are listed in Table II. All the links are characterized by a single-tap channel with line-of-sight capability.

In each simulation instance, the positions of the ISTAs are randomized, and all the nodes perform receiver-side synchronization and channel estimation in order to estimate the value of the time of arrival. As per the IEEE 802.11az standard, each I2R/R2I frame is associated with a secure preamble sequence (secure long training field [2]) that is generated using AES-128 in counter mode.

B. Simulation Results

Before analyzing the performance of the proposed enhancements, a comparison is made between the theoretical analysis for the position error bound and simulation results (that are averaged over a large number of instances). In Fig. 3, the position estimation error is plotted as a function of the average SNR per symbol and the number of symbol repetitions. For the sake of analysis, the parameters are assumed to be equal across all the ISTA-RSTA links (bandwidth of 20 MHz). The performance gap occurs due to erroneous estimation of the ToA, which in turn is a function of the sampling rate and random noise effects at the receiver. Naturally, the performance improves with increasing SNR, and the RMSE value approaches the PEB, which corroborates the asymptotic behaviour seen in estimation theory.

TABLE II: Simulation Parameters.

Parameter	**Value**	**Parameter**	**Value**
S_i	1, 2	t_{CTS}	4.6 μs
Average SNR per Symbol	12.2 dB (MCS=2) 25.7 dB (MCS=7)	t_{LMR}	14.1 μs
Bandwidth	20, 80 MHz	t_{NDPA}	9.5 μs
t_{TF}	10.8 μs	$D_{s,i}$	1500 bytes

The trade-off between the achievable position accuracy and latency/throughput is analyzed in Fig. 4. The SNR not only affects the position estimation accuracy, but also the achievable MCS and resultant data rate. A common SNR and bandwidth of 20 MHz is assumed at all the 4 ISTAs, while $S_1 = S_2 = 2$ and $S_3 = S_4 = 1$. For a given value of the position accuracy, the variation in the latency and throughput is significant between MCS 2 and 7. In addition to perceiving higher position accuracies, operating at a higher SNR also reduces the latency. It is interesting to note that the roll-off from the peak latency value to the flat region (wherein a single preamble symbol is sufficient) is highly steep in the case of MCS 7 and more gradual for MCS 2. This suggests that the gains realized from the optimization framework have a stronger impact for MCS 2 and improves the position accuracy drastically, while diminishing returns are obtained for MCS 7.

The impact of ISTA-grouping with asymmetric SNR and bandwidth values is analyzed in Fig. 5. Consider four ISTAs with $S_i = 1, \forall\, i$. Two of the ISTAs operate at MCS 2 (set 1), while the other two operate at MCS 7 (set 2). A performance comparison is made between three ISTA-grouping strategies.

- *Strategy 1:* In this strategy, the default approach is taken wherein all the ISTAs are grouped into a single ranging session. As can be inferred from Fig. 5a, the overall latency profile is 'symmetric' with respect to the range of positioning accuracies desired by both the sets. Naturally, set 2 can attain higher accuracies owing to a higher value of SNR. When a strict requirement is imposed by set 1 (say 18-20 cm), it is seen that the overall latency is further exacerbated. However, when a strict requirement is imposed by set 2 (say 4-5 cm), the increment in the latency is comparatively minimal. Hence, in such a grouping strategy, the high-SNR ISTAs are burdened by the low-SNR ISTAs, leading to higher latencies.
- *Strategy 2:* In this strategy, each of the sets is associated with its own Trigger Frame (TF) during the sounding phase. Each of the two TFs triggers the transmission of I2R frames from the ISTAs belonging to the respective set. Naturally, this leads to a marginal increase in the overall mean latency, but significantly reduces the latency

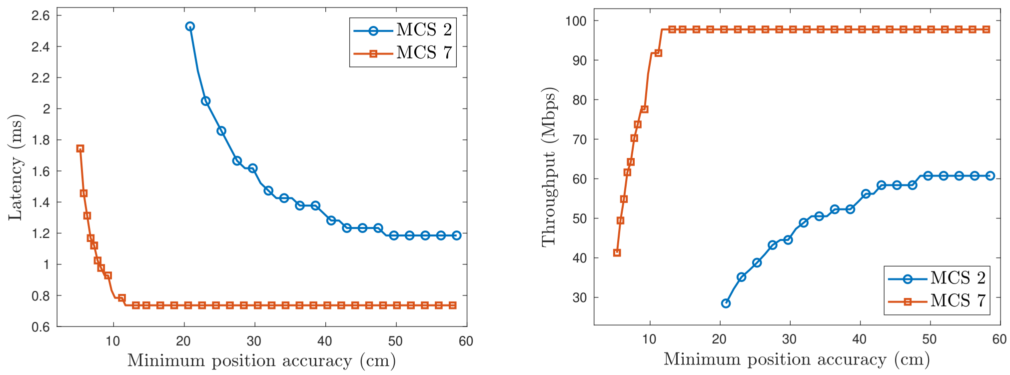

(a) Latency optimization under a positioning constraint.

(b) Throughput optimization under a positioning constraint.

Fig. 4: Tradeoff between the latency/throughput performance and positioning accuracy.

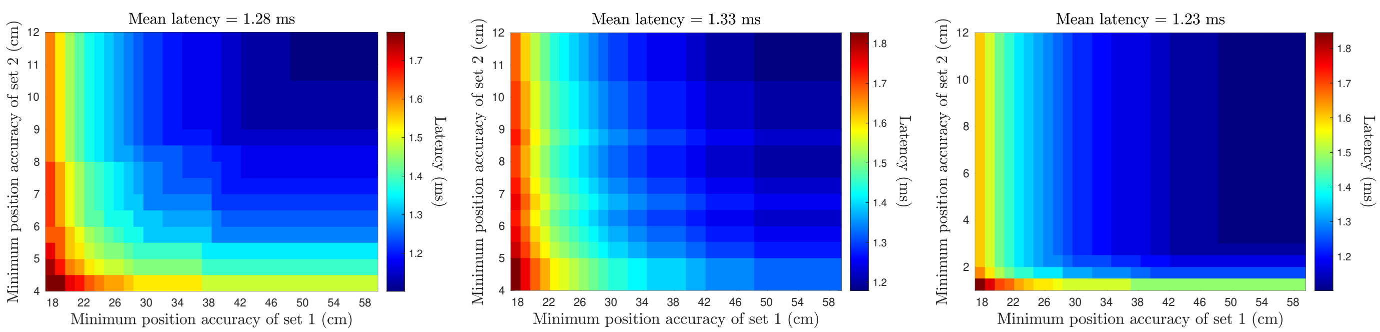

(a) Strategy 1.

(b) Strategy 2.

(c) Strategy 3.

Fig. 5: Performance comparison between user-grouping strategies as a function of the SNR and bandwidth.

when the accuracy requirement imposed by set 1 (with the lower MCS) is not stringent. However, for tighter requirements imposed by set 1, the performance is seen to be worse than scenario 1. Hence, this grouping strategy performs better than scenario 1, provided that set 1 does not require very high position accuracies.

- *Strategy 3:* The same approach of strategy 1 is applied, albeit with different *bandwidth* allocations for the sets. Let set 2 be allocated resource units amounting to 80 MHz for each of the ISTAs, while the allocation for set 1 remains at 20 MHz. The overall effect is a drastic reduction in the latency for both sets, which arises from the fact that set 2 needs fewer symbol repetitions to attain the same positioning accuracy at a higher bandwidth. However, this approach would require three 80 MHz channels to be available, as opposed to just one 80 MHz channel in the previous two approaches.

V. Conclusion

High-accuracy positioning systems will soon be prevalent in indoor scenarios. However, this comes at a cost to existing data-driven services. Various aspects of the trade-off between latency, throughput, and position estimation accuracy have been analyzed for a multi-user scenario using IEEE 802.11az. Through the development of an analytical framework, optimization problems are formulated and solved to yield the ideal number of preamble symbol repetitions that meet the desired requirements. Users operating at a higher SNR can obtain more accurate position estimates at lower latencies. Grouping strategies for users with asymmetric parameters have also been proposed to enhance the overall performance.

References

[1] F. Zafari, A. Gkelias, and K. K. Leung, “A survey of indoor localization systems and technologies,” *IEEE Communications Surveys & Tutorials*, vol. 21, no. 3, pp. 2568–2599, 2019.

[2] “IEEE Draft Standard for Information technology - Part 11: Wireless LAN Medium Access Control (MAC) and Physical Layer (PHY) Specifications - Amendment 4: Enhancements for positioning,” *IEEE P802.11az/D4.0*, pp. 1–282, October 2021.

[3] M. Z. Win, Y. Shen, and W. Dai, “A theoretical foundation of network localization and navigation,” *Proceedings of the IEEE*, vol. 106, no. 7, pp. 1136–1165, 2018.

[4] I. Martin-Escalona and E. Zola, “Passive round-trip-time positioning in dense IEEE 802.11 networks,” *Electronics*, vol. 9, no. 8, p. 1193, 2020.

[5] P. Figueiredo e Silva, V. Kaseva, and E. S. Lohan, “Wireless positioning in IoT: A look at current and future trends,” *Sensors*, vol. 18, no. 8, 2018.

[6] J. Henry, “Indoor Location : study on the IEEE 802.11 Fine Timing Measurement standard,” Thesis, Ecole nationale supérieure Mines-Télécom Atlantique, Dec. 2021.

[7] A. Makki, A. Siddig, and C. J. Bleakley, “Robust high resolution time of arrival estimation for indoor wlan ranging,” *IEEE Transactions on Instrumentation and Measurement*, vol. 66, no. 10, pp. 2703–2710, 2017.

[8] S. Lanzisera and K. S. J. Pister, “Burst mode two-way ranging with cramer-rao bound noise performance,” in *IEEE GLOBECOM 2008 - 2008 IEEE Global Telecommunications Conference*, 2008, pp. 1–5.

[9] S. Boyd and L. Vandenberghe, *Convex Optimization*. Cambridge University Press, 2004.

[10] J. Kronqvist, D. E. Bernal, A. Lundell, and I. E. Grossmann, “A review and comparison of solvers for convex MINLP,” *Optimization and Engineering*, vol. 20, no. 2, pp. 397–455, Jun 2019.